

Dispersion and Equalization in Fiber Optic Communication Systems

By D. M. HENDERSON

(Manuscript received July 2, 1973)

The additional optical power required at the repeater input in a fiber optic communication system due to intersymbol interference is experimentally measured. In the experiment, the intersymbol interference which results from differential mode delay in multimode fibers is minimized with a five-tap transversal equalizer. Error rate measurements are performed using five fibers ranging from 0.01 km to 1.25 km in length. In this manner, the additional optical power required to achieve a given error rate is found as a function of pulse width. The measured values compare favorably with the power penalties predicted by Personick. The trade-off between excess optical power and equalization penalty in dispersion-limited fiber systems is discussed.

I. INTRODUCTION

The temporal spreading of light pulses in an optical fiber can impose a limit on the highest data rate transmitted by a fiber optic communication system. Such spreading arises from differential mode delay in multimode fibers and material dispersion in both single-mode and multimode fibers.¹ The fiber materials and geometry together with the type of light source determine the magnitude of each effect. In this paper, we report the measurement of the additional optical power required to compensate for the loss in sensitivity resulting from the need to equalize detected light pulses that experience mode-delay spread. The experiment was carried out to determine the feasibility and practicality of equalization in dispersion-limited fiber systems.

In the experiment, light from a Burrus²-type gallium arsenide light-emitting diode (LED) digitally modulated at 48 Mb/s is coupled into a liquid-core fiber.³ Intersymbol interference in the detected pulse train is reduced with a transversal equalizer⁴ by forcing zero crossings in the pulse response at all sampling times but one. Error rate measure-

ments are made as a function of optical power on five sections of fiber ranging from 0.01 kilometer to 1.25 kilometers in length. From these measurements, the power required to assure a given error rate can be determined for the five pulse widths encountered. It is found that the measured power penalty due to intersymbol interference compares favorably with the values calculated by Personick.⁵ The trade-off between excess optical power and increased repeater spacing afforded by equalization is discussed in the concluding section of this paper.

II. DESCRIPTION OF EXPERIMENT

A block diagram of the experimental setup is shown in Fig. 1. For a source we use a Burrus-type diffused junction GaAs LED driven with a 48-Mb/s pseudorandom pulse stream. The LED output is first collimated, then attenuated as necessary with neutral-density filters, and finally focused onto the input of a liquid-core fiber. For the half-duty-cycle, return-to-zero, input light pulses used in the experiment, a maximum of -14.4 dBm average optical power can be coupled into the fibers.

In Table I, the measured loss and pulse width are shown for the five lengths of fiber used. The pulse width for the shortest section is deter-

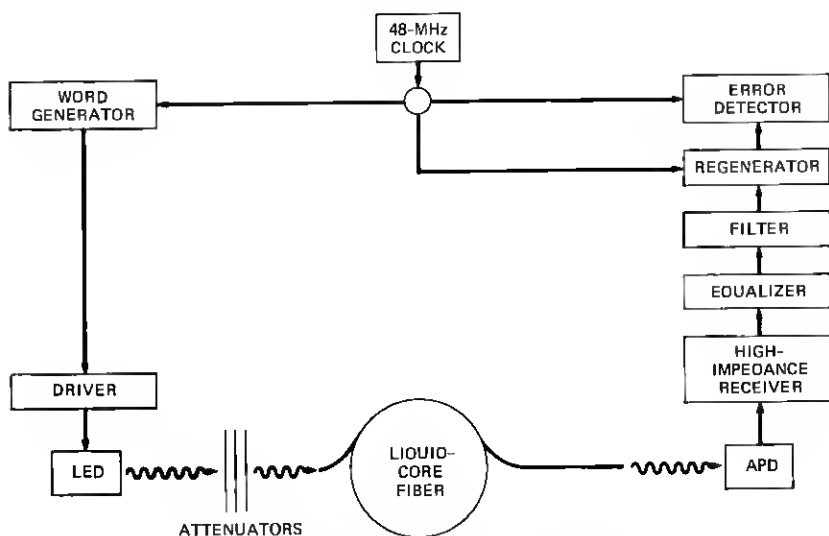


Fig. 1—Block diagram of experimental setup.

TABLE I—MEASURED LOSS AND PULSE WIDTHS FOR THE FIVE FIBERS TESTED

Fiber length (km)	Differential loss (dB/km)	Total loss (dB)	Rms pulse width (ns)
0.01	27.8	≈ 0	3.0
0.50	27.8	13.9	7.5
0.75	30.0	22.5	6.8
1.12	25.5	28.6	10.9
1.25	29.6	37.0	10.5

mined by the input pulse width and the bandwidth of the RCA C30817 avalanche photodiode (APD) detector. The additional width that is observed for the remaining four fibers is due to differential mode delay. Note that the 0.75-km fiber has greater differential loss and exhibits less pulse spreading than the fiber 0.50 km in length. Higher-order modes are presumably more highly attenuated in the 0.75-km fiber. The 1.25-km fiber is obtained by splicing the two together.

A high-impedance receiver is used, the first stage of which tends to integrate the detected light pulses. Incorporated in the receiver is an appropriate compensating network to assure that the receiver response is flat over the bandwidth of interest. Such a design has been shown to give improved signal-to-noise performance and reduced avalanche gain over a conventional, nonintegrating receiver.⁵ At near-optimal avalanche gain of ≈ 60 , a 10^{-9} error rate is realized with -53.7 dBm average optical power for the shortest section of fiber.

In order to equalize the detected optical pulses of various widths and shapes, a five-tap transversal equalizer is utilized. The tapped delay line with one time slot between taps is realized with RG188 coaxial cable. Variable gain and polarity of the signal picked off at each tap are achieved with MC1733 wideband differential amplifier integrated circuits. An additional wideband amplifier serves as a summing amplifier to recombine the signals. The equalizer is manually adjusted for each fiber tested.

Figure 2 shows the eye diagrams of the output of the "Nyquist" filter both with and without equalization for the shortest section of fiber. Here the equalizer serves to modify slightly the combined bandwidth response of receiver and filter, giving an improved response. The eye diagrams for the 1.12-kilometer fiber are shown in Fig. 3. In this case, differential mode delay has resulted in significant intersymbol interference. Adjusting the equalizer for zero crossings results in the equalized signal shown.

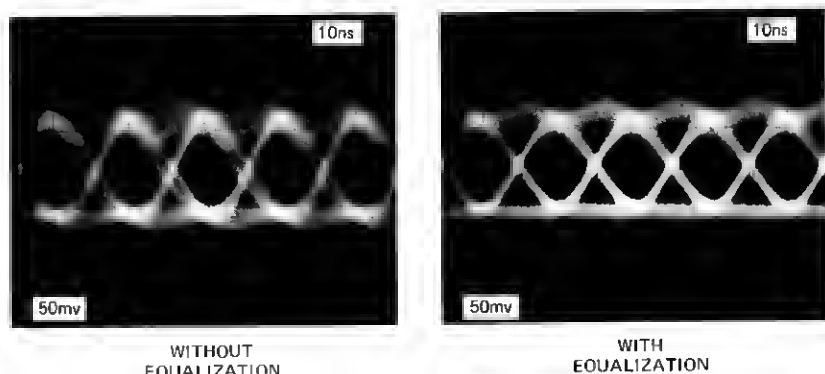


Fig. 2—Eye diagrams of input to regenerator with and without transversal equalizer for the 0.01-km fiber.

The equalized pulse train is regenerated and then compared with the original pseudorandom sequence in an error detector. Error rate measurements are then made as a function of optical power for each fiber. Optical power readings are taken with a Coherent Radiation Model 212 power meter.

III. RESULTS

The shape of the detected optical pulse strongly influences the amount of intersymbol interference and accordingly the additional optical power required. To accurately determine these shapes, a wideband, low-noise, 50-ohm amplifier is substituted for the high-impedance receiver. Through signal averaging with boxcar integration,

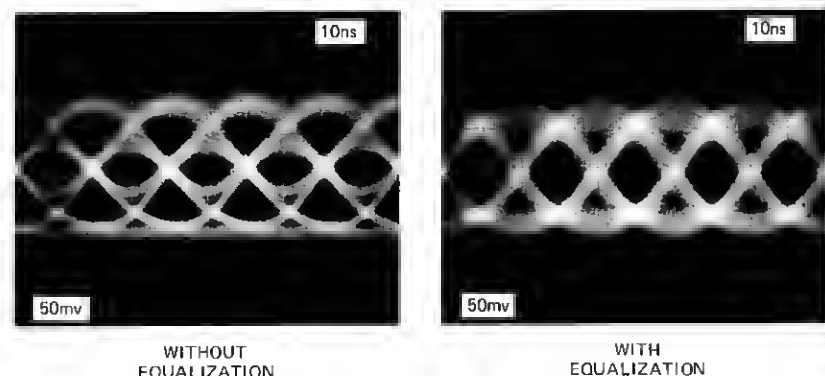


Fig. 3—Eye diagrams of the input to regenerator with and without transversal equalizer for the 1.12-km fiber.

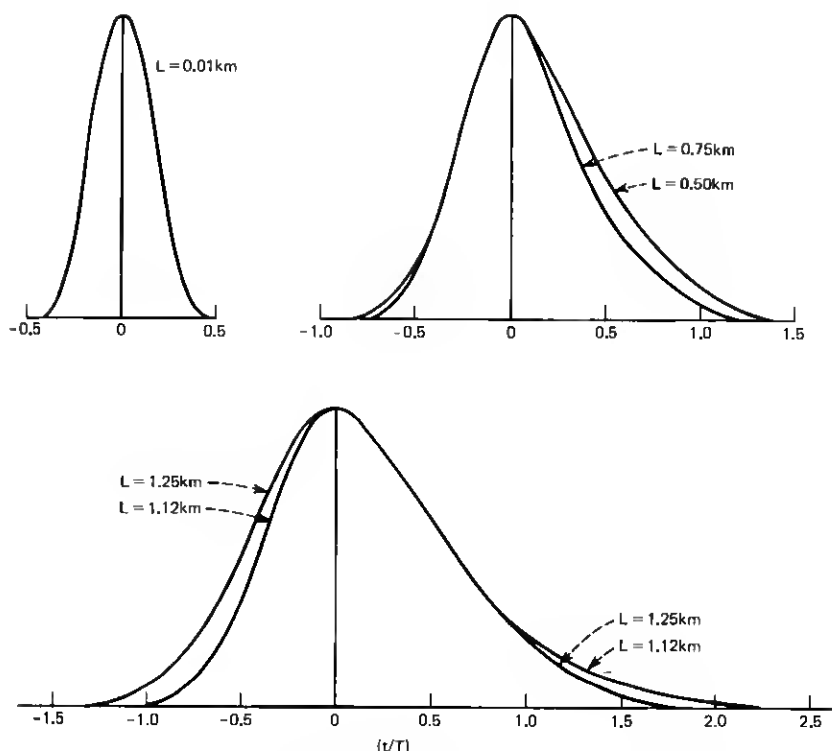


Fig. 4—Detected pulse shapes for the five fiber lengths tested.

the pulse shape can be recorded with signal-to-noise ratios in excess of 100. The pulse shapes for the five fiber lengths are plotted in Fig. 4 versus the normalized parameter t/T , where T represents one time slot (20.83 ns). From these data, the rms pulse widths σ of Table I were computed from the relation $\sigma^2 = [f t^2 f(t) dt] - [f t f(t) dt]^2$. Here $f(t)$ is the measured pulse shape normalized to unit area. The integration was numerically performed. In the figure, it is seen that for the shortest length, the pulse is confined to a single time slot. For the intermediate lengths the pulses are effectively confined to two time slots; for the longest lengths to three time slots.

A compilation of the error rate measurements is shown in Fig. 5. We have not attempted to fit the best curve to the data for each fiber. Instead we show superimposed on the data a curve of fixed shape which minimizes the deviation from the mean for all the fibers. The measured values fall within $\pm 1/8$ dB of the selected curve.

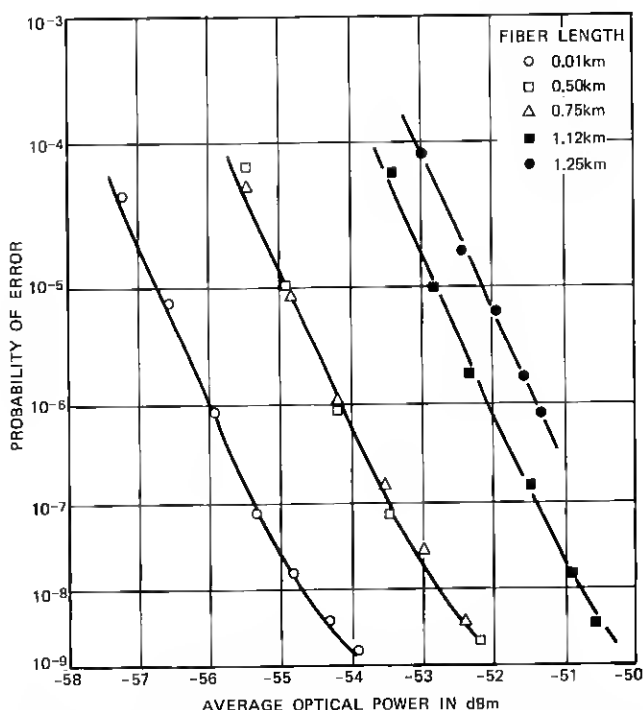


Fig. 5—Results of error rate measurements for the five fiber lengths tested.

The dependence of required optical power on the detected pulse width and shape has been calculated by Personick.⁶ In this calculation, the degradation in signal-to-noise ratio is found when equalizing from the detected pulse shape to a raised cosine shape. These results are presented in Fig. 6 in terms of the additional optical power required to maintain a fixed error rate. The dependence is shown for an exponential pulse $(1/\sigma) \cdot \exp(-t/\sigma)$ and a Gaussian pulse $(1/\sqrt{2\pi}\sigma) \cdot \exp(-t^2/2\sigma^2)$. When $(\sigma/T) < 0.25$ the power penalty for the two shapes is about equal. This behavior follows from the fact that little difference exists between the frequency spectra of the pulses over the range of interest ($0 < \omega/2\pi < 1/T$) in the narrow pulse limit. As the pulse width increases, the frequency spectrum of the Gaussian falls off much more rapidly than the exponential, resulting in a much larger power penalty.

Also shown are the measured points taken from Table I and Fig. 5. As no measurement is performed in the limit $\sigma/T \rightarrow 0$, the point at $\sigma/T = 0.15$ has been assigned the value of 0.25 dB to coincide with

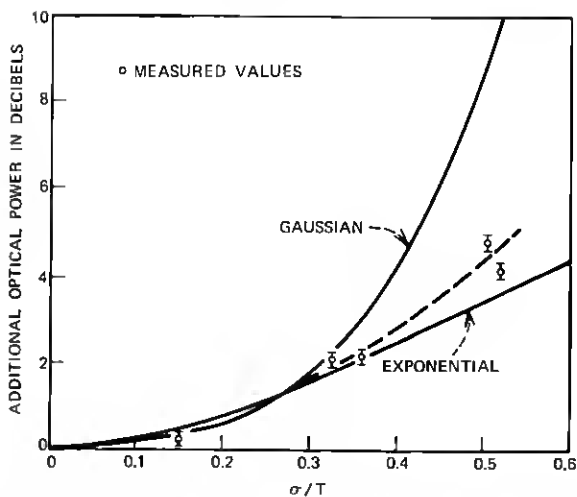


Fig. 6—The additional optical power required to maintain a fixed error versus normalized pulse width.

the Gaussian curve at that point because the measured pulse shape appears Gaussian rather than exponential. All other points have been scaled upward by this amount. Scaling this point to the value for the exponential pulse shape would merely shift all points up by an additional 0.12 dB and not affect the results significantly.

The measured points do not fall on a continuous curve but rather define a range of values. A dashed line which bisects the measured points is shown. It is interesting to note that the 0.75-km and 1.25-km fibers which lie above the dashed line have a more symmetric pulse shape and less of a tail than the 0.50-km and 1.12-km fibers which fall below the line. Such dependence is expected because the presence of the tail leads to spectra which fall off less rapidly in the frequency domain and therefore will suffer less power penalty. Calculations confirm this dependence.⁶

These results point out the important role the detected pulse shape plays. The decidedly asymmetric pulses that result from differential mode delay in liquid-core fibers lead to power penalties that increase much more slowly with pulse width than the penalty predicted from Gaussian pulses.

IV. DISCUSSION

In order to point out the benefits and limitations of equalization in dispersion-limited fiber optic communication systems, we treat a

specific case below. In the example, optical pulses from an LED source are transmitted by a low-loss fused-silica multimode fiber.

The fiber loss is considered first. Define

$$R(\text{dB}) = 10 \log [P_{\text{in}}/P_{\text{req}}(T_0)], \quad (1)$$

where P_{in} is the optical power coupled into the fiber and P_{req} is the power required in the absence of intersymbol interference to assure a given error rate at the data rate $1/T_0$. The distance $L(\text{km})$ over which one can communicate is governed by the fiber attenuation coefficient $\alpha(\text{dB/km})$ according to

$$R(T_0) - \alpha L \geq 0. \quad (2)$$

Consider the fused-silica multimode fiber announced by Corning Glass Works⁷ for which $\alpha = 4 \text{ dB/km}$ at $0.85 \mu\text{m}$. If we take for P_{req} the measured value of -53.7 dBm at 1 error in 10^{+9} and assume that -15 dBm can be launched into the fiber, then the inequality in eq. (2) would hold for distances less than $\approx 9.6 \text{ km}$. Additional signal-to-noise margin that is required would reduce this value in proportion to the fiber loss.

The required power is dependent on the data rate. For the high-impedance receiver it has been shown that⁵ $P_{\text{req}} \approx (T)^{-7/6}$. By defining $\tau = 10 \log (T_0/T)^{7/6}$, eq. (2) can be written

$$R(T_0) - \alpha L \geq \tau(T_0/T). \quad (3)$$

From this result the maximum separation can be found as a function of data rate. In Fig. 7 the curve marked 4 dB/km loss shows the dependence. The inequality is satisfied for distances L below the line.

Personick, et al.,⁸ have studied the pulse spreading in such a low-loss fused-silica multimode fiber excited by an LED source. For a fiber with a tailored index-of-refraction profile which gives an effective numerical aperture of 0.12 and an effective diameter of $96 \mu\text{m}$, they find that material dispersion is the dominant pulse-spreading mechanism due to the large spectral width (400 \AA) of the LED. The measured rms pulse width is found to be $\sigma/L \equiv \sigma' = 1.75 \text{ ns/km}$.

If we do not equalize, but restrict the pulse width to avoid intersymbol interference, then an additional limit is imposed on L . As an example, take the arbitrary restriction $\sigma' \cdot L/T < 0.35$. In Fig. 7, this inequality is satisfied to the left of the curve marked material dispersion. Therefore, the area in the lower left-hand side bound by the two limiting curves shows the available working distances versus data rate. It should be noted that another possible way to reduce this

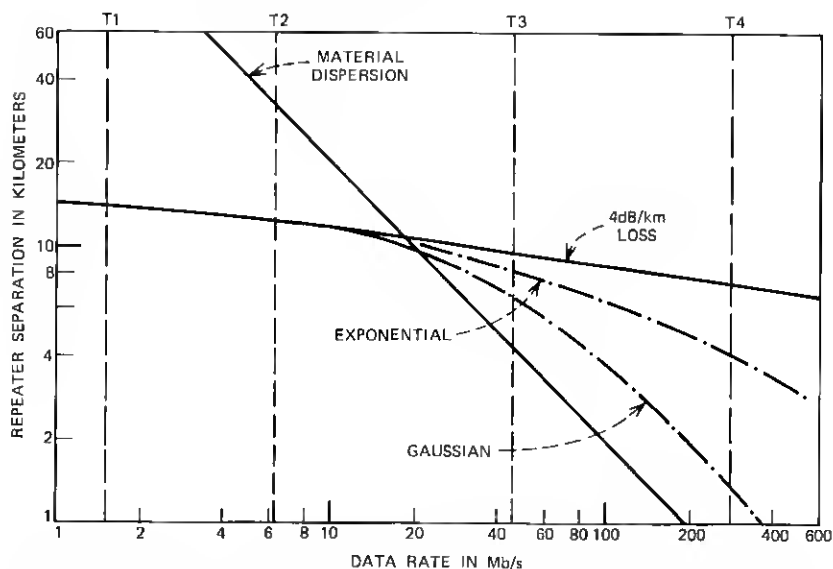


Fig. 7—Maximum repeater spacing versus data rate for the fiber system described in text.

dispersion is to trade off optical power and LED bandwidth by reducing the spectral width of the output. We deal with equalization alone in this paper.

At higher data rates, dispersion limits the repeater spacing before the fiber loss limit occurs. Below we consider the effect of using this excess power for equalization to increase the spacing. The power penalty has been presented as a function of pulse width in Fig. 6. Here σ/T become $\sigma'L/T$. Let $p(L, T)$ expressed in dB represent the power penalty. Equation (3) then becomes

$$R(T_0) - \alpha L \geq \tau(T_0/T) + p(L, T). \quad (4)$$

The solutions to this equation are shown in Fig. 7 for both the Gaussian and exponential pulses. At the data rate used in this experiment (48 Mb/s) the repeater separation is increased from ≈ 4.2 km to ≈ 6.5 km for the Gaussian-shaped pulses. At that distance the rms pulse width is $\sigma/T \cong 0.55$. For exponential pulses the spacing could be as large as 8.4 km with accompanying pulse width $\sigma/T = 0.70$. The exact distance will depend strongly on the detailed shape of the detected pulses as noted previously. In any case, increases of at least

50 percent would be possible. At higher data rates the potential increases are greater still.

V. SUMMARY

We have experimentally measured the additional optical power that is required to maintain a fixed error rate for digitally modulated light pulses that encounter differential mode delay in multimode fibers. The resulting power penalty versus pulse width compares favorably with the values predicted by Personick. We find that the asymmetric shape of the mode-delay-spread pulses results in penalties which increase much more slowly with pulse width than does the penalty predicted for Gaussian pulses. Each potential dispersion-limited fiber system must be examined separately to determine the potential increase in repeater spacing that equalization offers as the pulse spreading mechanisms vary significantly among different sources and fibers. The example presented shows graphically how one can utilize excess optical power in equalizing delay distortion and thereby maximize the repeater spacing for a given data rate.

VI. ACKNOWLEDGMENTS

The author wishes to express his appreciation to J. S. Cook, S. D. Personick, and J. Stone for many helpful discussions. Peter K. Runge generously furnished the high-impedance receiver. The technical assistance of A. R. McCormick was invaluable.

REFERENCES

1. Cloge, D., "Dispersion in Weakly Guiding Fibers," *Appl. Opt.*, **10**, No. 11 (November 1971), pp. 2442-2445.
2. Burrus, C. A., and Miller, B. I., "Small-Area, Double-Heterostructure Aluminum-Gallium Arsenide Electroluminescent Diode Source for Optical-Fiber Transmission Lines," *Opt. Commun.*, **4**, No. 4 (December 1971), pp. 307-309.
3. Stone, J., "Optical Transmission in Liquid-Core Quartz Fibers," *Appl. Phys. Lett.*, **20**, No. 7 (April 1972), pp. 239-240.
4. Lucky, R. W., Salz, J., and Weldon, E. J., Jr., *Principles of Data Communication*, New York: McGraw-Hill, 1968, pp. 128-165.
5. Personick, S. D., "Receiver Design for Digital Fiber Optic Communication Systems," *B.S.T.J.*, **52**, No. 6 (July-August 1973), pp. 843-886.
6. Personick, S. D., private communication.
7. Keck, D. B., Mauer, R. D., and Schultz, P. C., "On the Ultimate Lower Limit of Attenuation in Glass Optical Waveguides," *Appl. Phys. Lett.*, **22**, No. 7 (April 1973), pp. 307-309.
8. Personick, S. D., Hubbard, W. M., Gloge, D., Holden, W. S., Dawson, R. W., Ghinnock, E. L., and Lee, T. P., "Measurements of Material Dispersion in Optical Fibers," presented at the Conference on Laser Engineering and Applications, Washington, D. C., May 30-June 1, 1973.